

On the Ionisation Fraction in Protoplanetary Disks II: The Effect of Turbulent Mixing on Gas-phase Chemistry

Martin Ilgner and Richard P. Nelson

Astronomy Unit, Queen Mary, University of London, Mile End Road, London E1 4NS, U.K.

Received 21 July 2005 / Accepted 30 August 2005

Abstract. We calculate the ionisation fraction in protostellar disk models using two different gas-phase chemical networks, and examine the effect of turbulent mixing by modelling the diffusion of chemical species vertically through the disk. The aim is to determine in which regions of the disk gas can couple to a magnetic field and sustain MHD turbulence. The disk models are conventional α -disks, and the primary source of ionisation is X-ray irradiation from the central star. We assume that the vertical mixing arises because of turbulent diffusion, and accordingly equate the vertical diffusion coefficient, \mathcal{D} , with the kinematic viscosity, ν .

We find that the effect of diffusion depends crucially on the elemental abundance of heavy metals (magnesium) included in the chemical model. In the absence of heavy metals, diffusion has essentially no effect on the ionisation structure of the disks, as the recombination time scale is much shorter than the turbulent diffusion time scale. When metals are included with an elemental abundance above a threshold value, the diffusion can dramatically reduce the size of the magnetically decoupled region (“dead zone”), or even remove it altogether. This arises when recombination is dominated by metal ions, and the recombination time exceeds the vertical diffusion time scale. For a complex chemistry the elemental abundance of magnesium required to remove the dead zone is $x_{\text{Mg}} = 10^{-10} - 10^{-8}$. We also find that diffusion can modify the reaction pathways, giving rise to dominant species when diffusion is switched on that are minor species when diffusion is absent. This suggests that there may be chemical signatures of diffusive mixing that could be used to indirectly detect turbulent activity in protoplanetary disks.

We find examples of models in which the dead zone in the outer disk region is rendered deeper when diffusion is switched on. This is caused by turbulent mixing diluting the electron fraction in regions where the ionisation degree is marginally above that required for good coupling.

Overall these results suggest that global MHD turbulence in protoplanetary disks may be self-sustaining under favourable circumstances, as turbulent mixing can help maintain the ionisation fraction above that necessary to ensure good coupling between the gas and magnetic field.

Key words. accretion, accretion disks – MHD - planetary systems: protoplanetary disks – stars: pre-main sequence

1. Introduction

Observational studies of young stars in star forming regions indicate that protostellar disks are a common occurrence (e.g. Beckwith & Sargent 1996; Prosser et al. 1994). Many disks show signatures of active accretion, with the probability of accreting disks being present, and the apparent gas accretion rate, scaling inversely with the age of the stellar system in which the young stars are embedded. The canonical value for the gas accretion rate, however, is often quoted as being $\dot{M} \sim 10^{-8} M_{\odot} \text{ yr}^{-1}$ (e.g. Sicilia-Aguilar et al. 2004).

There are a number of potential mechanisms that may lead to angular momentum transport in protostellar disks, giving rise to the observed mass accretion. Angular momentum transport that occurs globally throughout the disk, producing accretion at the observed rates, probably requires turbulence to act as a source of anomalous vis-

cosity. At the present time the only source of turbulence in accretion disks that is known to work is the magnetorotational instability (MRI), which gives rise to MHD turbulence (Balbus & Hawley 1991; Hawley & Balbus 1991; Hawley, Gammie & Balbus 1996).

As has been well documented in the literature, there are continuing questions about the applicability of the MRI to protostellar disks because of their high densities and low temperatures that lead to low levels of ionisation (e.g. Balbus & Balbus 1994; Gammie 1996). Magnetohydrodynamic simulations of disks including ohmic resistivity (Fleming, Stone & Hawley 2000) show that for magnetic Reynolds numbers Re_m smaller than a critical value Re_m^{crit} , turbulence cannot be sustained and the disks return to a near-laminar state. Typically the gas-phase electron fraction should be $x[e^-] \simeq 10^{-12}$ for disks to be able to sustain MHD turbulence.

A number of studies of the ionisation fraction in protostellar disks have appeared in the literature. Gammie (1996) suggested that disks may have magnetically “active zones” sustained by thermal or cosmic ray ionisation, adjoining regions that were magnetically inactive – “dead zones”. More recent studies have examined this issue in greater depth. Sano et al. (2000) used a more complex chemical model that included dust grains. Glassgold et al. (1997) and Igea et al. (1999) examined the role of X-rays as a source of ionisation in protoplanetary disks. Fromang et al. (2002) considered the role of heavy metals in determining the ionisation fraction because of the potential importance of charge-transfer reactions. Matsumura & Pudritz (2003) examined the ionisation fraction in the externally heated, passive disk model proposed by Chiang & Goldreich (1997) using the Sano et al. (2000) chemical reaction network. Semenov et al. (2004) recently studied disk chemistry using a complex reaction set drawn from the UMIST database.

In a recent paper (Ilgner & Nelson 2005 – hereafter “paper 1”), we examined and compared the predictions made by a number of chemical reaction networks about the ionisation fraction in standard α -disk models. This study included an examination of the reaction scheme proposed by Oppenheimer & Dalgarno (1974), and more complex schemes drawn from the UMIST database, in addition to a number of gas-grain chemical networks. In this paper we extend this initial study to examine the role of turbulent mixing in determining the ionisation fraction in protoplanetary disk models using gas-phase chemistry. We consider the simple Oppenheimer & Dalgarno (1974) model, and a more sophisticated chemical reaction network based on the UMIST database. We allow the vertical diffusion of each chemical species to occur, equating the diffusion coefficient \mathcal{D} to the kinematic viscosity ν that drives disk accretion. We find that the inclusion of diffusion can have a very significant effect on the ionisation structure of protoplanetary disks, in particular when a small abundance of heavy metals (magnesium) is introduced into the reaction networks. In some cases the disk can modify the ionisation fraction sufficiently that the dead zone disappears entirely.

This paper is organised as follows. In section 2 we describe the chemical models, our implementation of the diffusion equation for chemical species, and the numerical method used to solve the reaction-diffusion equations. In section 3 we discuss the various models that we compute and present their results. In section 4 we summarise our main findings and discuss their potential consequences for protoplanetary disks.

2. Reaction-diffusion model

We consider a system of s chemical species whose local abundances in the protoplanetary disk evolve due to chemical reactions and vertical diffusive transport, arising because of concentration gradients and driven by turbulence. In the discussion below we define r to be the number of

chemical reactions, and n to be the total molar density (expressed in units of mols cm^{-3}). The global elemental composition of the system is conserved by applying appropriate boundary conditions in our reaction-diffusion model.

2.1. Disk models

The underlying disk models considered are standard α -disks. Details are given in paper 1 and references therein. To recap: the disks are assumed to orbit a young solar mass star and undergo viscous evolution. We use the α prescription for the viscous stress, such that the kinematic viscosity $\nu = \alpha c_s^2 / \Omega$, where c_s is the sound speed and Ω is the local Keplerian angular velocity. Heating of the disk is provided by viscous dissipation alone, and cooling by radiation transport in the vertical direction. The disk structure is obtained by solving for hydrostatic and thermal equilibrium. We employ 30 zones in the vertical direction (from midplane to disk surface) and 100 zones in radius between $0.1 \leq R \leq 10$ AU when computing the chemical evolution. The underlying disk model was computed using 100 cells in the vertical direction, and values were interpolated onto the 30 grid points used in computing the chemistry. The disk models are completely specified by the mass accretion rate, \dot{M} and the value of α . We consider two models: one with $\dot{M} = 10^{-7} M_\odot \text{ yr}^{-1}$ and $\alpha = 10^{-2}$, the other with $\dot{M} = 10^{-8} M_\odot \text{ yr}^{-1}$ and $\alpha = 5 \times 10^{-3}$. The mass contained in these models is $0.0087 M_\odot$ and $0.0049 M_\odot$ respectively. Contour plots showing the distribution of the kinematic viscosity, ν , are shown in figures 1 and 2.

2.2. Kinetic model

We have applied two different kinetic models for the gas-phase chemistry. The first is a simple five component model introduced originally by Oppenheimer & Dalgarno (1974). The second is a much more sophisticated reaction scheme based on the UMIST database (Le Teuff et al. 2000). We assume that ionisation of the disk material arises because of incident X-rays that originate in the corona of the central T Tauri star. We neglect contributions from Galactic cosmic rays as they are not expected to penetrate into inner disk regions we consider due to the stellar wind. The details of these models have been described in paper 1, where they were given the labels `model11` and `model13`. We maintain this labelling scheme in this paper so as to establish continuity with our previous work.

The kinetic equations obey the law of atomic balance:

$$\sum_{i=1}^s \nu_{ij} = 0, \quad (j = 1, 2, \dots, r). \quad (1)$$

Here ν_{ij} divided by the molecular mass M_i of the i^{th} component (defined in units of grams/mol) is proportional to the stoichiometric coefficient, while the i^{th} species is involved in the j^{th} chemical reaction. The molar density, n_i ,

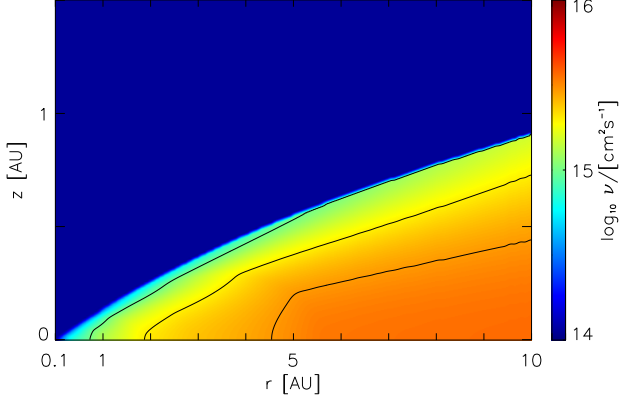


Fig. 1. The kinematic viscosity ν ; the contour lines refer to values $1 \times 10^{15}, 2 \times 10^{15}, 3 \times 10^{15} \text{ cm}^2\text{s}^{-1}$. The disk parameters are $\alpha = 10^{-2}$ and $\dot{M} = 10^{-7} \text{ M}_{\odot}\text{yr}^{-1}$.

of the i^{th} component is related to the mass density, ρ_i , of the i^{th} component through

$$\rho_i = M_i n_i. \quad (2)$$

The rate of change of the molar density of the i^{th} component within a given volume due to chemical reactions and flow of species i into that volume is

$$\frac{\partial n_i}{\partial t} = -\nabla \cdot (n_i \mathbf{v}_i) + \sum_{j=1}^r \nu_{ij} J_j. \quad (3)$$

J_j denotes the chemical reaction rate associated with the j^{th} chemical reaction, while $\nu_{ij} J_j$ is the formation/destruction rate of the i^{th} component due to the j^{th} chemical reaction. \mathbf{v}_i is the velocity of the i^{th} component.

2.3. Diffusion

The first term on the right hand side of equation (3) represents the rate of flow of species i into a given volume. In this paper we assume that the underlying protoplanetary disk is turbulent, and that turbulent diffusion acts to transport chemical species from one region of the disk to another. As we are primarily interested in how diffusion affects the ionisation fraction of the disk material, and we expect the largest gradients in the electron fraction to be in the vertical (z) direction, we consider only vertical diffusion in the paper. Equation (3) becomes

$$\frac{\partial n_i}{\partial t} = \frac{\partial}{\partial z} \left(n \mathcal{D} \frac{\partial x_i}{\partial z} \right) + \sum_{j=1}^r \nu_{ij} J_j, \quad (i = 1, \dots, s) \quad (4)$$

where \mathcal{D} is the turbulent diffusion coefficient, and $x_i = n_i/n$ is the fractional abundance of species i . We present a fuller discussion of the derivation of equation (4) in appendix. A similar set of equations has been used by numerous authors who have examined the effect of turbulent

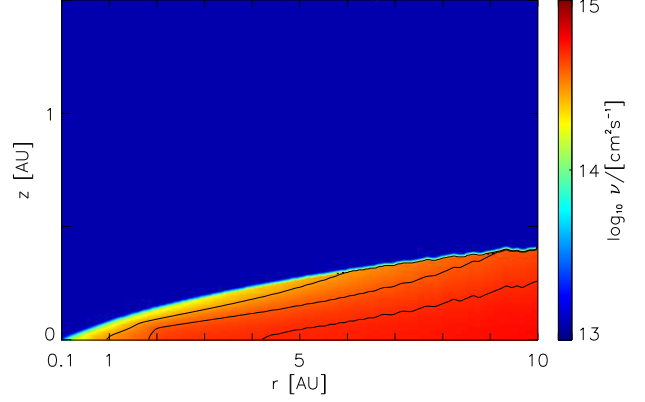


Fig. 2. The kinematic viscosity ν ; the contour lines refer to values $3 \times 10^{14}, 4 \times 10^{14}, 5 \times 10^{14} \text{ cm}^2\text{s}^{-1}$. The disk parameters are $\alpha = 5 \times 10^{-3}$ and $\dot{M} = 10^{-8} \text{ M}_{\odot}\text{yr}^{-1}$.

diffusion on the chemical state of molecular clouds (Xie, Allen & Langer 1995; Rawlings & Hartquist 1997; Willacy, Langer & Allen 2002) and on the role of radial mixing in protoplanetary disks (Wehrstedt & Gail 2002, 2003). In this work we adopt the approximation that $\mathcal{D} = \nu$, where ν is the kinematic viscosity that drives the radial diffusion of mass through the protostellar accretion disk. Although there is still some debate about the precise relationship between the vertical diffusion coefficient and the effective kinematic viscosity that arises because of MHD turbulence in astrophysical disks (see Carbillado, Stone & Pringle 2005; Johansen & Klahr 2005), it is not expected that \mathcal{D}/ν differs greatly from unity. As already discussed, the basic kinetic models that we consider in this paper are models `model11` and `model13` described in paper 1. When these kinetic models are used in conjunction with turbulent mixing we use the labels `model11D` and `model13D`, respectively. When diffusion is switched off we often use the term “pure kinetic models” when describing the results in later sections.

2.4. Numerical method

The reaction–diffusion model is governed by the set of s coupled parabolic partial differential equations (4). These equations can be interpreted as a linear superposition of two operators, one describing the mass transfer of species i due to diffusion, and the other describing changes due to chemical reactions. There are number of possible approaches to solving these equations. We employed the method of lines, which is a technique used, e.g., in atmospheric physics that solves the full system of equations simultaneously (e.g. Chang et al. 1974), rather than a more usual operator splitting approach. Hence, we transformed the system of s PDEs into a system of $s \times nz$ ODEs, where nz is the number of grid points in the z direction. Adopting a uniform mesh along this coordinate direction,

we replaced the spatial derivative in equation (4) by a finite differencing scheme.

The boundary conditions are taken to be symmetric at $z = 0$ (disk midplane) and no flux at $z = H$ (photospheric disk height) for all times t . Applying the Crank–Nicholsen finite differencing scheme and the chosen boundary conditions satisfy the conservation of elements and charges at any cylindrical radius R . Using $nz = 30$, we found that the elements and charges are conserved at all cylindrical radii and for all times t . At $t \leq 10^5$ yrs, for example, the change in both the elemental abundances and the total charge was below 10^{-8} per cent compared with the corresponding values at $t = 0$ yr.

We have allowed all species, including molecular hydrogen and helium, to be mixed by diffusion. We thus checked *a posteriori* if the assumed constancy of the mean molecular weight $\mu = 2.33$ is satisfied. We find that it is, as expected from the fact that the value of μ is dominated by hydrogen and helium, and these species do not develop significant concentration gradients, thus precluding significant diffusion.

We also allowed free electrons to be mixed by diffusion. Differences in the concentration gradients of the ions and electrons can in principle lead to different diffusion velocities which may result in a non-zero diffusion flux of charges per zone. We found, however, that this did not occur.

2.5. Initial conditions

The reaction–diffusion calculations are initiated with all chemical elements being in neutral atomic form, apart from hydrogen which is assumed to be in molecular form. The species were distributed in the disk uniformly. Details are given in paper 1. Chemical changes lead to concentration gradients that then initiate the action of diffusion.

3. Results

We have evolved the disk chemistry using the kinetic models described in section 2.2, including mixing due to turbulent diffusion. The primary aim of this work is to compare and understand the differences in the distribution of free electrons that arise in the different models, and in particular to understand the role that turbulent mixing plays in determining the free electron fraction and distribution. We wish to determine which parts of the disk are sufficiently ionised for the gas to be well coupled to the magnetic field, and thus able to maintain MHD turbulence, and which regions are too neutral for such turbulence to be maintained. We refer to those regions as being “active” and “dead” zones respectively, with the region bordering the two being the “transition” zone. The important discriminant that determines whether the disk is active or dead is the magnetic Reynolds number, Re_m , defined by

$$Re_m = \frac{Hc_s}{\mu_m} \quad (5)$$

where H is the disk semi-thickness, c_s is the sound speed, and μ_m is the magnetic diffusivity (not to be confused with the mean molecular weight). Numerical simulations (e.g. Fleming, Stone & Hawley 2000) indicate that a critical value of the magnetic Reynolds number, Re_m^{crit} , exists such that non linear MHD turbulence cannot be sustained if Re_m falls below Re_m^{crit} . We adopt a value of $Re_m^{\text{crit}} = 100$ in this paper, following the value used in paper 1 and Fromang et al. (2002). We are able to calculate the distribution of Re_m within our disks. Regions with $Re_m < 100$ are deemed to be magnetically dead, and those with $Re_m > 100$ magnetically active.

When it comes to diffusion we consider the two extremes with the diffusion coefficient $\mathcal{D} = \nu$ and $\mathcal{D} = 0$. Models with $\mathcal{D} = \nu$ are labelled **model1D** and **model3D**. Models with $\mathcal{D} = 0$ reduce to the pure kinetic models **model1** and **model3** already discussed in paper 1.

We solved the equations by integrating over a time interval of 100,000 yrs. Hence, the ionisation fraction $x[e^-]$ is a function of time t , and in principle so is the location of the transition zone. For all kinetic models, however, the change in the vertical location of the transition zone at all cylindrical radii in the computational domain was below the grid resolution for $t > 50,000$ yrs.

3.1. Diffusion versus Recombination

In order for diffusion to modify the ionisation fraction of material near the transition zone in protoplanetary disks, and hence modify the size of the dead zone, the vertical diffusion time should be less than the recombination time for free electrons.

We consider diffusion across a scale height at $R \simeq 5$ AU in the heavier disk model. The scale height of this disk is given by $H/R \simeq 0.1$ (see paper 1). Figure 1 shows that the kinematic viscosity at 5 AU is $\nu \simeq 3 \times 10^{15} \text{ cm}^2 \text{ s}^{-1}$, which we adopt as the value for the vertical diffusion coefficient \mathcal{D} . The diffusion time is given by

$$\tau_{\mathcal{D}} = \frac{H^2}{\mathcal{D}} = 625 \text{ yrs.} \quad (6)$$

We consider a simple chemistry (described in detail in section 3.2) involving a representative molecule and its ion, “m” and “m⁺”, and a representative heavy metal and its ion, “M” and “M⁺”. In regions well shielded from X-rays, the recombination rate of free electrons is given by

$$\frac{dx[e^-]}{dt} = -k_1 x[e^-] x[m^+] N[H_2] - k_2 x[e^-] x[M^+] N[H_2] \quad (7)$$

where k_1 is the rate coefficient for recombination between molecular ions and electrons, k_2 is the equivalent for heavy metal ions, and $N[H_2]$ is the number density of hydrogen molecules. The two scenarios of interest are the metal-free case and the metal-dominated case.

In the metal-free case, where the electron fraction $x[e^-] = x[m^+]$, equation (7) becomes

$$\frac{dx[e^-]}{dt} = -k_1 x^2[e^-] N[H_2]. \quad (8)$$

Table 1. Rate coefficients applied for the Oppenheimer & Dalgarno model. The values are always used as reference values.

ζ	ζ_{eff}	s^{-1}
$\tilde{\alpha}$	$3 \times 10^{-6}/\sqrt{T}$	$\text{cm}^3 \text{s}^{-1}$
$\tilde{\beta}$	3×10^{-9}	$\text{cm}^3 \text{s}^{-1}$
$\tilde{\gamma}$	$3 \times 10^{-11}/\sqrt{T}$	$\text{cm}^3 \text{s}^{-1}$

Assuming $N[\text{H}_2]$ remains constant, equation (8) integrates to give the recombination time

$$\tau_{\tilde{\alpha}} = \frac{1}{k_1 N[\text{H}_2]} \left[\frac{1}{x_{e-}^f} - \frac{1}{x_{e-}^i} \right], \quad (9)$$

where x_{e-}^i and x_{e-}^f are the initial and final values of x_{e-} during diffusion over a scale height. At $R = 5$ AU, the electron abundance at the transition zone is $x_{e-}^f = 5 \times 10^{-13}$, as shown in figure 7 of paper 1. The rate coefficient $k_1 = \tilde{\alpha}$, $N[\text{H}_2] \simeq 5 \times 10^{12} \text{ cm}^{-3}$, and $T \simeq 100$ K (see figures 1 and 2 in paper 1). The recombination time is then $\tau_{\tilde{\alpha}} \simeq 15$ days. It is clear that diffusion is not expected to have a significant impact on the dead zone structure in this case.

The rate coefficient appropriate to the metal-dominated case is $k_2 = \tilde{\gamma}$, which gives a recombination time of $\tau_{\tilde{\gamma}} \simeq 4200$ yrs. Comparing this with the diffusion time $\tau_D = 625$ yrs, it is clear that a protoplanetary disk with a significant population of gas-phase heavy metals should have the structure of the dead zone modified substantially by the action of turbulent diffusion.

3.2. Oppenheimer & Dalgarno model

The underlying kinetic model of **model1D** involves two elements, five species/components, and four reactions. These species are free electrons “ e^- ”, a representative molecule “ m ”, a heavy metal atom “ M ”, and their ionized counterparts “ m^+ ” and “ M^+ ”. The rate coefficients for the ionisation of m and for dissociative recombination of m^+ are given by ζ and $\tilde{\alpha}$, while the rate coefficients $\tilde{\beta}$ and $\tilde{\gamma}$ apply to the charge-transfer reaction between m^+ and M and the radiative recombination of M^+ , respectively. The rate coefficients are listed in table 1 and were used in all **model1D** calculations unless stated otherwise. Results obtained in paper 1 showed that the dead zones obtained using **model1** were always smaller than those obtained for the complex models. We find it useful, however, to analyse **model1** and **model1D** as many of the features of this simple model can be helpful in understanding the more complex model.

The results obtained for **model1D** are presented in figure 3, which shows the column density of the whole disk plotted as a function of radius using the solid line, and the column density of the active zone only using either dotted lines (for which $D = 0$) or dashed lines (for which $D = \nu$).

The first thing to note is that diffusive mixing makes essentially no difference to the size of the active zone when

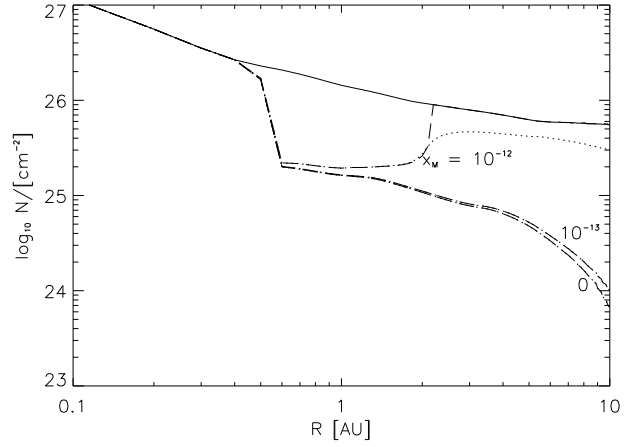


Fig. 3. - **model1(D)** - Column densities of the whole disk (solid line) and of the active zones (dashed and dotted lines) - referring to magnetic Reynolds numbers greater than 100 - for different values x_M . While the dashed lines refer to simulation with $D = \nu$, the dotted lines refer to simulations with $D = 0$. The reference values for the rate coefficients are applied. The disk parameters are $\alpha = 10^{-2}$ and $\dot{M} = 10^{-7} \text{ M}_{\odot} \text{yr}^{-1}$.

heavy metals are not included in the chemistry. This is illustrated by the lowest line plotted in figure 3, which appears as a dash-dotted line in the figure, but is actually a dashed line (representing the case with diffusion switched on) plotted over a dotted line (representing the case when diffusion is switched off). The reason for this result is simple: the recombination time when metals are absent is very much shorter than the turbulent mixing time. As a parcel of fluid moves from the active region of the disk toward the dead zone, free electrons will recombine with molecular ions rapidly, making no change to the ionisation fraction of the dead region.

Increasing the heavy metal elemental abundance from zero to $x_M = 10^{-13}$ and switching diffusion on also makes no difference to the size of the dead zone. The addition of such a small fraction of metals does not prevent recombination between molecular ions and electrons being the dominant destruction process of the free electrons. This is illustrated by the second lowest line in figure 3.

Increasing the heavy metal fraction to $x_M = 10^{-12}$ results in a significant change in the structure of the dead zone when diffusion is switched on. Interior to $R \leq 2$ AU there is almost no change in the size of the active zone because recombination between electrons and molecular ions is still the dominant process determining the ionisation fraction. Beyond $R \geq 2$ AU, however, the dead zone disappears completely when diffusion is switched on, whereas as a dead zone remains when $x_M = 10^{-12}$ and $D = 0$. The reason for this difference is simple. The charge-transfer reaction between molecular ions and neutral heavy metals removes most of the molecular ions beyond $R \geq 2$ AU. This allows the recombination between metal ions

and electrons to become the primary means by which free electrons are destroyed. The recombination time for this reaction, however, is much longer than for recombination between molecular ions and electrons, and is also longer than the turbulent mixing time. As a parcel of fluid moves from the active zone toward the dead zone, the time it takes is shorter than the time scale over which the free electrons are destroyed, thus increasing the free electron fraction in the dead zone and allowing it to become active.

In order to explore further the role played by the relative diffusion and recombination time scales, and to examine conditions under which the reaction–diffusion model deviates from the pure kinetic model, we have performed some numerical experiments in which we have artificially modified recombination times. We discuss these briefly below.

Case: $x_M = 0$

In this case, `model1D` reduces to a three component system with two reactions. The molecular ion m^+ and the free electron e^- are formed and destroyed by the same chemical reaction. Since m^+ and e^- are mixed with the same diffusion velocity, it is simple to demonstrate how the mixing time scale, τ_D , and the molecular ion–electron recombination time scale, $\tau_{\tilde{\alpha}}$, affect the ionisation fraction $x[e^-]$ (where $\tau_D \propto 1/\nu$ and $\tau_{\tilde{\alpha}} \propto 1/\tilde{\alpha}$). We systematically changed the ratio $\tau_D/\tau_{\tilde{\alpha}}$ by changing the rate coefficient $\tilde{\alpha}$ of the molecular ion – electron recombination reaction. We find that the recombination time scale $\tau_{\tilde{\alpha}}$ has to be increased by three orders of magnitude before the results of the reaction–diffusion model `model1D` deviates from the pure kinetic model `model11`. This illustrates the basic point that reasonable diffusion rates will be unable to change the size of the dead zone obtained using the Oppenheimer & Dalgarno model in the absence of heavy metals in the gas phase.

Case: $x_M \neq 0$

We performed a similar exercise to that just described, but included heavy metals with an elemental concentration of $x_M \geq 10^{-12}$. This value causes the recombination of metal ions with free electrons to dominate over recombination with molecular ions beyond $R \geq 2$ AU. We used the reference values for the rate coefficients $\tilde{\alpha}$ and $\tilde{\beta}$ listed in table 1, and modified systematically the recombination rate coefficient $\tilde{\gamma}$ between metals and electrons only. $\tau_{\tilde{\gamma}} \propto 1/\tilde{\gamma}$ now becomes the dominant recombination time scale. Figure 3 shows that the addition of metals with $x_M \geq 10^{-12}$ causes a substantial difference between the reaction–diffusion model and the pure kinetic model. We find that we need to decrease the value of $\tau_{\tilde{\gamma}}$ by two orders of magnitude in order that diffusion has no impact on the size of the dead zone.

One can consider this issue in reverse, and ask what changes need to be made to $\tau_{\tilde{\gamma}}$ in the pure kinetic model `model11` in order for it to give the same sized dead zone as `model1D` with $\mathcal{D} = \nu$ and the standard value of $\tilde{\gamma}$. We find that if $\tau_{\tilde{\gamma}}$ is increased by two orders of magni-

tude in `model11` then the resulting dead zone is the same as obtained in the standard `model1D`. For this particular reaction network, this indicates that diffusion acts as an effective reduction in the dominant recombination rate coefficient.

3.3. UMIST model

The underlying kinetic model in `model3D` was constructed by extracting all species and reactions from a given species set of 174 species and the UMIST database containing the elements H, He, C, O, N, S, Si, Mg, Fe. 1965 reactions were extracted from the UMIST database. A full description is given in paper 1. Compared with the previous model of Oppenheimer & Dalgarno (`model1D`) there are now many pathways through which free electrons can recombine with molecular ions, each with their own associated time scale. Without knowing *a priori* which ion is dominant, it is difficult to make estimates of the relative mixing and recombination time scales. Indeed, our previous study presented in paper 1 suggests that there is more than one dominant ion that determines the ionisation fraction, complicating the picture further.

An additional complication is that the introduction of diffusion into the kinetic model can modify the chemical pathways, such that comparing the products of the pure kinetic models with those of the reaction–diffusion models becomes difficult. This effect manifests itself in our study by changing the identities of the molecular ions which are dominant in the transition region between dead and active zones.

We now discuss the results obtained using `model3D`, beginning with models for which the heavy metal, magnesium, was neglected from the chemical network, before discussing the effects that including Mg has on the ionisation fraction and resulting dead zone structure.

Case: $x_{Mg} = 0$

We begin by discussing the results of `model3D` applied to the disk model defined by $\alpha = 10^{-2}$ and $\dot{M} = 10^{-7} \text{ M}_{\odot} \text{ yr}^{-1}$ before discussing the results obtained in the disk model with $\alpha = 5 \times 10^{-3}$ and $\dot{M} = 10^{-8} \text{ M}_{\odot} \text{ yr}^{-1}$. As a general result we find that the location of the transition zone (which separates the active and the dead zones) is very similar when comparing the results obtained for both disk models by applying a reaction–diffusion model with $\mathcal{D} = \nu$ and $\mathcal{D} = 0$, respectively. This is illustrated by figure 4 in which the column density of the whole disk is plotted using the solid line, the column density of the active zone obtained using the pure kinetic model is plotted using the dotted line, and the results of the reaction–diffusion model are plotted using the dashed line. We see that `model3D` with $\mathcal{D} = \nu$ produces a slightly larger active zone within $0.6 \leq R \leq 3$ AU, but beyond this region the depth of the active zone is unaffected by diffusive mixing.

We have examined the abundances of the key molecular ions in the transition region between the active and dead zones. Typically the ionisation balance is not deter-

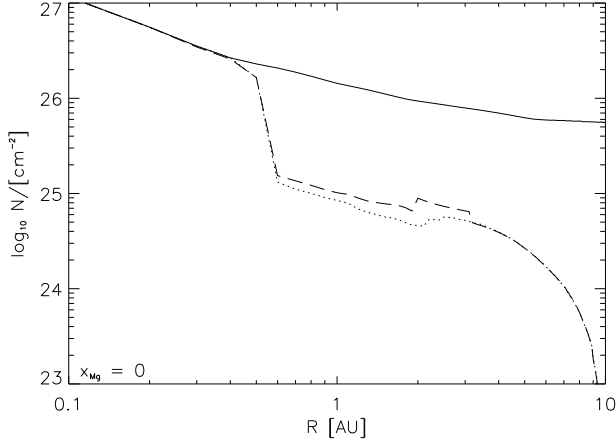


Fig. 4. - model13(D) - Column densities of the whole disk (solid line) and of the active zones (dashed and dotted lines) - referring to magnetic Reynolds numbers greater than 100 - for $x_{\text{Mg}} = 0$. While the dashed line refers to simulations with $\mathcal{D} = \nu$, the dotted line refers to simulation with $\mathcal{D} = 0$. The disk parameters are $\alpha = 10^{-2}$ and $\dot{M} = 10^{-7} \text{ M}_{\odot} \text{ yr}^{-1}$.

mined by a single dominant ion, but by a small number of ions. We find clear differences between the pure kinetic model and the reaction–diffusion model in those regions in radius where there is the greatest difference in the depth of the active zone between the two models.

HCNH^+ and NH_4^+ are the most abundant ions in the neighbourhood of the transition zone between $1.8 \leq R \leq 3.0 \text{ AU}$ obtained for the pure kinetic model. It is important to note that the ratio between both ion concentrations does not change gradually in the vicinity of the transition zone, but instead there is a sharp transition: above the transition zone HCNH^+ is more abundant than NH_4^+ by one order of magnitude. This ratio becomes inverted just below the transition zone by the same order of magnitude. Due to the significantly shorter recombination time scale, electrons recombine more efficiently with NH_4^+ than with HCNH^+ . Hence, NH_4^+ determines the location of the transition zone rather than HCNH^+ .

By contrast, the abundance of NH_4^+ is significantly lowered by applying the reaction–diffusion model with $\mathcal{D} = \nu$. Now, the more complex ion $\text{H}_4\text{C}_2\text{N}^+$ is two orders of magnitude the more abundant than the next most abundant ion CH_3OH_2^+ . In addition, since mixing tends to reduce the concentration gradients of each species with height, z , the ratio between both ion concentrations $x[\text{H}_4\text{C}_2\text{N}^+]/x[\text{CH}_3\text{OH}_2^+]$ changes gradually when passing through the transition zone. In the same region between $1.8 \leq R \leq 3 \text{ AU}$ we found significant differences in the distribution of most of the species obtained for a reaction–diffusion model and the corresponding pure kinetic model. This is a clear indication that mixing may change the kinetics significantly.

We now consider the $\alpha = 5 \times 10^{-3}$, $\dot{M} = 10^{-8} \text{ M}_{\odot} \text{ yr}^{-1}$

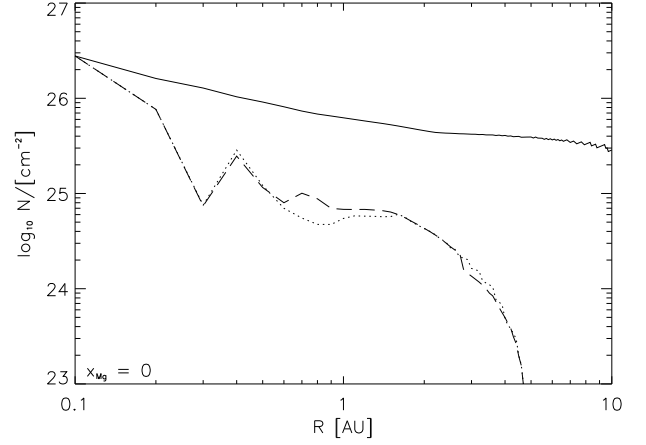


Fig. 5. - model13(D) - Column densities of the whole disk (solid line) and of the active zones (dashed and dotted lines) - referring to magnetic Reynolds numbers greater than 100 - for $x_{\text{Mg}} = 0$. While the dashed line refers to simulations with $\mathcal{D} = \nu$, the dotted line refers to simulation with $\mathcal{D} = 0$. The disk parameters are $\alpha = 5 \times 10^{-3}$ and $\dot{M} = 10^{-8} \text{ M}_{\odot} \text{ yr}^{-1}$.

disk model. The results for this model are shown in figure 5. We first note that this disk model generates an intrinsically deeper dead zone in the outer regions of the disk beyond $R \geq 3 \text{ AU}$, even though the ionisation rate due to X-rays is higher due to the smaller surface density. This is a temperature effect that arises because the viscous heating is reduced because of the smaller α and \dot{M} values. The recombination rates scale according to $k \propto 1/\sqrt{T}$, leading to a lower ionisation fraction.

We focus in particular on locations $0.6 \leq R \leq 1.1 \text{ AU}$ where the most significant differences in the vertical depth of the active zone appear when comparing the reaction–diffusion model and the corresponding pure kinetic model.

The most abundant ions produced by the pure kinetic model in the neighbourhood of the transition zone are $\text{H}_4\text{C}_2\text{N}^+$ and NH_4^+ . These species are similarly abundant, but the recombination time for electrons with NH_4^+ is much shorter than with $\text{H}_4\text{C}_2\text{N}^+$, so NH_4^+ determines the position of the transition zone. The corresponding reaction–diffusion model again results in $x[\text{NH}_4^+]$ dropping significantly so that it no longer controls the ionisation fraction in the neighbourhood of the transition zone. Instead, $\text{H}_4\text{C}_2\text{N}^+$ is the most abundant molecular ion, being one order of magnitude more abundant than the next most abundant ion H_3O^+ . This is again evidence that the presence of turbulent mixing in a protoplanetary disk can change the reaction kinetics. This leads to the intriguing possibility that such changes may in the future act as observational diagnostics for the presence of turbulence in disks.

Case: $x_{\text{Mg}} \neq 0$

We now consider the effect that including magnesium has

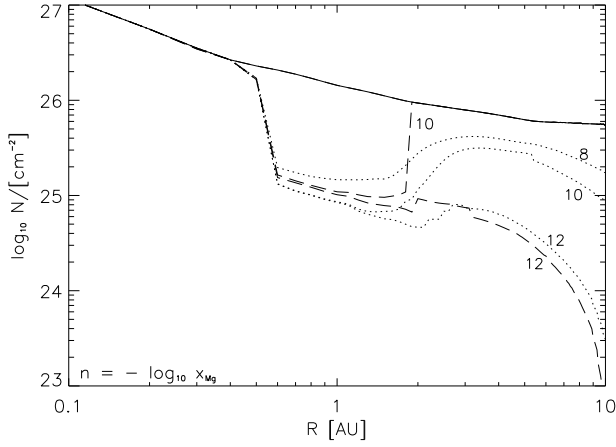


Fig. 6. - **model13(D)** - Column densities of the whole disk (solid line) and of the active zones (dashed and dotted lines) - referring to magnetic Reynolds numbers greater than 100 - for different values of x_{Mg} . While the dashed lines refer to simulations with $\mathcal{D} = \nu$, the dotted lines refer to simulations with $\mathcal{D} = 0$. Especially, for a reaction-diffusion model with $\mathcal{D}_{\text{eff}} = \nu$ no dead zones are observed above values $x_{\text{Mg}} \geq 10^{-8}$. The disk parameters are $\alpha = 10^{-2}$ and $\dot{M} = 10^{-7} \text{ M}_{\odot} \text{ yr}^{-1}$.

on the models. We begin by discussing the results obtained for the disk model with $\alpha = 10^{-2}$, $\dot{M} = 10^{-7} \text{ M}_{\odot} \text{ yr}^{-1}$. The results for **model13D** are shown in figure 6. The dotted lines show the column density of the active zones obtained by the pure kinetic model for various values of x_{Mg} . The dashed lines show the column density of the active zones obtained by the reaction-diffusion model. In general we find that mixing affects the size of the active zone significantly as soon as metals with concentrations above a threshold value are involved.

The addition of magnesium with elemental concentration $x_{\text{Mg}} = 10^{-12}$ makes very little difference to the size of the dead zone, whether diffusion is switched on or not, as seen by comparing figures 4 and 6. This is because a low value of x_{Mg} does not allow Mg^+ to become the dominant ion *via* charge-transfer reactions.

Increasing the magnesium elemental abundance to $x_{\text{Mg}} \geq 10^{-10}$ changes the picture dramatically when diffusion is switched on. The pure kinetic models with these magnesium abundances included contain no regions in the disk beyond $R \geq 0.4 \text{ AU}$ where the disk is fully active, although the dead zone tends to shrink beyond $R \geq 2 \text{ AU}$. In this region Mg^+ followed by HCNH^+ are the most dominant ions, while in the region $0.4 \leq R \leq 2 \text{ AU}$ the NH_4^+ ion is dominant. The reaction-diffusion model **model13D** with $\mathcal{D} = \nu$ and $x_{\text{Mg}} = 10^{-10}$ produces a dead zone of similar depth to the pure kinetic model between radii $0.4 \leq R \leq 2 \text{ AU}$. The identity of the dominant molecular ion in this region changes, however, when diffusion is switched on. The abundances of HCNH^+ and NH_4^+ are found to decrease significantly, and are replaced by the ion $\text{H}_4\text{C}_2\text{N}^+$. The

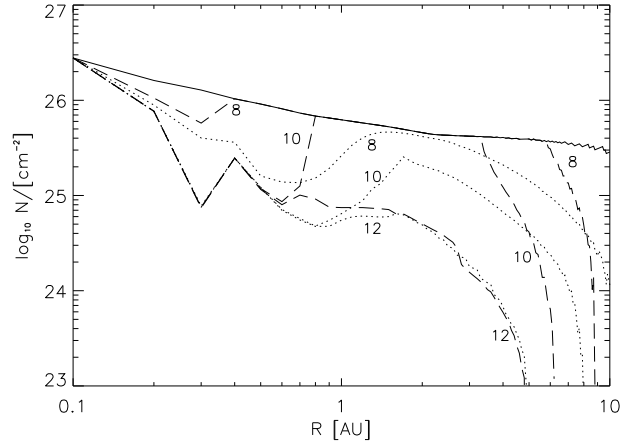


Fig. 7. - **model13(D)** - Column densities of the whole disk (solid line) and of the active zones (dashed and dotted lines) - referring to magnetic Reynolds numbers greater than 100 - for different values of x_{Mg} . While the dashed lines refer to simulations with $\mathcal{D} = \nu$, the dotted lines refer to simulations with $\mathcal{D} = 0$. The disk parameters are $\alpha = 5 \times 10^{-3}$ and $\dot{M} = 10^{-8} \text{ M}_{\odot} \text{ yr}^{-1}$.

disk is rendered fully active beyond $R \geq 2 \text{ AU}$ where Mg^+ is the dominant ion and the recombination time increases above the mixing time.

model13D with $\mathcal{D} = \nu$ and $x_{\text{Mg}} = 10^{-8}$ produces a fully active disk, in contrast to the corresponding pure kinetic model **model13**. For these higher magnesium abundances, Mg^+ becomes the dominant ion through the charge-transfer reaction with molecular ions, and the abundance of NH_4^+ is much reduced. The long electron recombination time associated with Mg^+ allows diffusive mixing to maintain a disk that is fully active.

We now consider the disk model with $\alpha = 5 \times 10^{-3}$, $\dot{M} = 10^{-8} \text{ M}_{\odot} \text{ yr}^{-1}$. The results are presented in figure 7, where the column density of the active zones obtained using the pure kinetic models are plotted using dotted lines. Dashed lines represent the column density of active zones obtained using the reaction-diffusion model.

Adding magnesium with an elemental abundance $x_{\text{Mg}} = 10^{-12}$ results in very little change in the size of the dead zone whether diffusion is switched on or not (compare figures 5 and 7).

Increasing the magnesium elemental concentration to $x_{\text{Mg}} = 10^{-10}$ causes substantial changes to occur when diffusion is switched on. Interior to $R \leq 0.7 \text{ AU}$ there is no change because the molecular ions NH_4^+ and $\text{H}_4\text{C}_2\text{N}^+$ are dominant over Mg^+ there, both with and without diffusive mixing. Between $0.7 \leq R \leq 3 \text{ AU}$ the disk becomes fully active when diffusion is switched on, but maintains a significant dead zone there in the pure kinetic model. The influence of Mg^+ allows the recombination time to be increased so that mixing can render the disk active. Beyond $R \geq 5 \text{ AU}$ we obtain the surprising result that diffusive mixing causes the depth of the dead zone to in-

crease rather than decrease. The reason for this is that the ionisation fraction at large radii in the pure kinetic model is always close to the critical value for the disk to be active. The addition of diffusion appears to have a diluting effect on the electron fraction in the active zone, which causes the dead zone to increase in size.

Increasing the magnesium elemental concentration to $x_{\text{Mg}} = 10^{-8}$ causes further changes to occur when diffusion is switched on. The Mg^+ ion is dominant throughout the disk, and the disk model is rendered entirely active between the radii $0.4 \leq R \leq 6$ AU. We again find that the dead zone becomes deeper at radii beyond $R \geq 8$ AU when diffusive mixing is effective. The reason is the same as given above: the ionisation fraction at these radii is always close to the critical value required to render the disk active. Diffusive mixing dilutes the electron fraction there, producing a deeper dead zone.

4. Summary

We have presented the results of calculations that examine the ionisation fraction in protoplanetary disks models. Our models compute the chemical evolution of the gas, with X-rays from the central star being the primary source of ionisation, and also include vertical diffusion of the chemical species. This diffusion is designed to mimic the effects of turbulent mixing arising from the MHD turbulence that is thought to drive accretion in protostellar disks (e.g. Balbus & Hawley 1991).

The main findings of this work are:

- The simple Oppenheimer & Dalgarno (1974) kinetic model produces smaller dead zones than a more complete kinetic model based on the UMIST database. This is true whether diffusion is switched on or not.
- All models which did not include heavy metals (magnesium) give rise to substantial dead zones. The inclusion of diffusion in these cases makes very little difference to the size and depth of the dead zone. This is because the recombination of molecular ions with electrons occurs too rapidly for turbulent mixing to be effective.
- The addition of heavy metals (magnesium) to the reaction networks can give rise to dramatic changes in the sizes of dead zones when diffusion is included. This is because the recombination time between metal ions and electrons is orders of magnitudes longer than that between molecular ions and electrons, and is longer than the diffusive mixing time. The addition of metals, combined with charge-transfer reactions, removes most of the molecular ions and replaces them with the longer lived metal ions.
- For the Oppenheimer & Dalgarno (1974) network, the addition of heavy metals with fractional abundance $x_{\text{M}} = 10^{-12}$ leads to the dead zone disappearing beyond $R \geq 2$ AU when diffusion is switched on. In the absence of diffusion a substantial dead zone exists in this region of this disk.

- For the model based on the UMIST database, the addition of magnesium to the chemical network with a fractional abundance of $x_{\text{Mg}} = 10^{-10}$ leads to the dead zone disappearing beyond $R \geq 2$ AU when diffusion is switched on. When the abundance of magnesium is increased to $x_{\text{Mg}} = 10^{-8}$ the dead zone disappears completely. Models in which diffusion is not present, but with the same magnesium abundances have substantial dead zones.
- We find that the changes in the size of dead zones when diffusion is switched on do not only arise because free electrons are mixed into the dead zone, but also because the chemical pathways are modified by diffusion. One effect of this in our models is that the dominant ions near the transition zone between dead and active zones change their identity when diffusion is initiated. This raises the interesting possibility that there may be chemical signatures of turbulent diffusion that can act potentially as observational diagnostics of turbulence in protoplanetary disks.
- For some disk models, the inclusion of diffusion can cause the dead zone depth to increase in the outer regions of the disk. This arises because these particular models predict that the electron fraction is only slightly above the critical value for the disk to be active in these regions when diffusion is switched off. Switching diffusion on can dilute the electron fraction in these regions, leading to a deeper dead zone.

Overall, our models indicate that turbulence in protoplanetary disks can be a self-sustaining process, providing that certain criteria are met, and indicate that dead zones can be reduced or removed altogether through turbulent mixing processes. These criteria are:

- (i) There are sufficient magnesium atoms available in the gas phase so that recombination between magnesium ions and electrons becomes the dominant process by which the local ionisation fraction is determined.
- (ii) The turbulent diffusion time scale is shorter than the dominant recombination time on which free electrons are removed.

A potentially serious omission from our models is the existence of small dust grains. These are known to sweep up free electrons (and metal atoms) very efficiently, and when included with the interstellar abundance they substantially increase the size and depth of dead zones in protoplanetary disks (see Sano et al 2000; paper 1). It is very likely that these grains will need to be substantially depleted by grain growth before the effects of turbulent mixing described in this paper are realised, as the removal rate of electrons from the gas phase is too large to allow diffusion to be effective.

An interesting question is whether a disk that has a substantial dead zone, and which is subject to a temporary period of intense ionisation (by large X-ray flares of the type recently reported by Feigelson et al. 2005, for example), can enter into a self-sustaining turbulent state in which the turbulent mixing maintains a fully active

disk. This question is currently under investigation and will be the subject of a future publication. An equally interesting question is whether a disk with a substantial dead zone, sandwiched between active zones near the disk surface, can become globally active due to turbulent motions overshooting into the dead zone and transporting free electrons into it. This question cannot be addressed by calculations of the type presented in this paper, but their results suggest that this may be possible under certain circumstances.

Acknowledgements. This research was supported by the European Community's Research Training Networks Programme under contract HPRN-CT-2002-00308, "PLANETS".

References

- Sicilia-Aguilar, A., Hartmann, L., Briceño, C., Muzerolle, J., Calvet, N., 2004, *AJ*, **128**, 805–821
- Balbus, S., Hawley, J., 1991, *ApJ*, **376**, 214–222
- Beckwith, S. and Sargent, A., 1996, *Nature*, **383**, 139–144
- Bird, R., Stewart, W., Lightfoot, E., 1960, *Transport Phenomena* (New York, London, Sydney: Wiley)
- Blaes, O., Balbus, S., 1994, *ApJ*, **421**, 163–177
- Carballido, A., Stone, J., Pringle, J., 2005, *MNRAS*, **358**, 1055–1060
- Chang, J., Hindmarsh, A., Madsen, N., 1974, in *Stiff differential systems*, ed. R. Willoughby (New York and London: Plenum Press), 51
- Chiang, E., Goldreich, P., 1997, *ApJ*, **490**, 368–376
- Feigelson, E., Getman, K., Townsley, L., Garmire, G., Preibisch, Th., Grosso, N., Montmerle, T., Muench, A., McCaughrean, M., 2005, *astro-ph/0506503*
- Fleming, T., Stone, J., Hawley, J., 2000, *ApJ*, **530**, 464–477
- Fromang, S., Terquem, C., Balbus, S., 2002, *MNRAS*, **329**, 18–28
- Gammie, C., 1996, *ApJ*, **457**, 355–362
- Glassgold, A., Najita, J., Igea, J., 1997, *ApJ*, **480**, 344–350
- Hawley, J., Balbus, S., 1991, *ApJ*, **376**, 223–233
- Hawley, J., Gammie, C., Balbus, S., 1996, *ApJ*, **464**, 690–703
- Igea, J., Glassgold, A., 1999, *ApJ*, **518**, 848–858
- Ilgner, M., Nelson, R., 2005, *A&A*, **in Press**,
- Johansen, A., Klahr, H., 2005, *astro-ph/0501641*
- Le Teuff, Y., Millar, T., Markwick, A., 2000, *A&AS*, **146**, 157–168
- Matsumura, S., Pudritz, R., 2003, *ApJ*, **598**, 645–656
- Oppenheimer, M., Dalgarno, A., 1974, *ApJ*, **192**, 29–32
- Prosser, C., Stauffer, J., Hartmann, L., Soderblom, D., Jones, B., Werner, M., McCaughrean, M., 1994, *ApJ*, **421**, 517–541
- Rawlings, J., Hartquist, T., 1997, *ApJ*, **487**, 672–688
- Sano, T., Miyama, S., Umebayashi, T., Nakano, T., 2000, *ApJ*, **543**, 486–501
- Semenov, D., Wiebe, D., Henning, Th., 2004, *A&A*, **417**, 93–106
- Wehrstedt, M., Gail, H., 2002, *A&A*, **385**, 181–204
- Wehrstedt, M., Gail, H., 2003, *A&A*, **410**, 917–935
- Willacy, K., Langer, W., Allen, M., 2002, *ApJ*, **573**, L119–L122
- Xie, T., Allen, M., Langer, W., 1995, *ApJ*, **440**, 674–685

Appendix A:

The diffusion flow \mathbf{J}_i^a of the i^{th} component may be expressed in various ways depending which reference velocity \mathbf{v}^a is used. The molar diffusion flow \mathbf{J}_i^a is

$$\mathbf{J}_i^a = n_i (\mathbf{v}_i - \mathbf{v}^a). \quad (\text{A.1})$$

The reference velocities \mathbf{v}^a are defined as weighted averages of the velocity \mathbf{v}_i of the i^{th} component

$$\mathbf{v}^a = \sum_{i=1}^s a_i \mathbf{v}_i, \quad \left(\sum_{i=1}^s a_i = 1 \right) \quad (\text{A.2})$$

with a_i as normalised weights.

Since the mass is conserved, the diffusion fluxes of the s components are not independent. Specifying the reference velocity \mathbf{v}^a by the mean molar velocity \mathbf{v}^m

$$\mathbf{v}^m = \sum_{i=1}^s x_i \mathbf{v}_i \quad (\text{A.3})$$

where x_i denotes the molar fraction of the i^{th} component

$$x_i = \frac{n_i}{n}, \quad \left(\sum_{i=1}^s n_i = n \right) \quad (\text{A.4})$$

the molar diffusion fluxes are constrained by

$$\sum_{i=1}^s \mathbf{J}_i^m = 0. \quad (\text{A.5})$$

There are several contributions to the diffusion flux. We assume that the most important contribution to the diffusion flux is caused by concentration gradients rather than due to pressure gradients, external forces, and coupled effects (cross-effects). Diffusion caused by concentration gradients is called “ordinary” diffusion. Considering ordinary diffusion processes only, we often use the phrase “diffusion” instead of “ordinary” diffusion. The (ordinary) diffusion is described by the phenomenological equation, which is well-known as Fick’s first law for a binary system $s = 2$. By analogy to the molar diffusion flow for a binary system, we define an effective molar diffusion flow $\mathbf{J}_{\text{eff},i}^m$ for the diffusion of the i^{th} component in a mixture by

$$\mathbf{J}_{\text{eff},i}^m = -n \mathcal{D}_{\text{eff},i} \nabla x_i. \quad (\text{A.6})$$

The effective binary diffusivity $\mathcal{D}_{\text{eff},i}$ for species i in a mixture can be calculated from the diffusivity \mathcal{D}_{ij} of the pair $i-j$ in a binary mixture by applying the so-called “Stefan–Maxwell equation”. Especially, for systems in which all the \mathcal{D}_{ij} are the same $\mathcal{D}_{\text{eff},i}$ is now given by

$$\mathcal{D}_{\text{eff},i} = \mathcal{D}_{ij}. \quad (\text{A.7})$$

Because of the definition of the molar diffusion flow \mathbf{J}_i^a , see equation (A.1), the velocity of the i^{th} component and the reference velocity \mathbf{v}^a are related to each other. In particular, in a molar diluted system¹ we deal with, one can approximate the reference velocity by $\mathbf{v}_i^a = \mathbf{v}^m = 0$. Similiar

¹ i.e. for $n_i \ll 1$, $i = 1, 2, \dots, s-1$, $n_s \sim 1$

applies for mass diluted systems with $\mathbf{v}_i^a = \mathbf{v}_n = 0$ where \mathbf{v}_n denotes the n^{th} component velocity. This is in agreement with the hydrostatic equilibrium assumption in z direction. Finally, equation (3) can be simplified by:

$$\frac{\partial n_i}{\partial t} = \frac{\partial}{\partial z} \left(n \mathcal{D}_{\text{eff},i} \frac{\partial}{\partial z} x_i \right) + \sum_{j=1}^r \nu_{ij} J_j, \quad (i = 1, \dots, s) \quad (\text{A.8})$$

constraint by equation (A.5). Note that we simplified the symbol for the effective binary diffusivity for species i in a mixture by using \mathcal{D} instead of $\mathcal{D}_{\text{eff},i}$.

Because of the molar diluted system we consider and due to the fact that the most abundant components (which are molecular hydrogen and helium) do not contribute to the molar diffusion fluxes, the mass is conserved even by neglecting equation (A.5).